IEEE Access
Multidisciplinary | Rapid Review | Open Access Journal

Received September 14, 2021, accepted October 12, 2021, date of publication October 15, 2021, date of current version October 26, 2021.

Digital Object Identifier 10.1109/ACCESS.2021.3120711

Investigating the Axonal Magnetic Fields Corresponding to Delta and Theta Waves in the Human Brain Using Direct Detection MRI

LI SZE CHOW[1], REUBEN GEORGE[1], MOHAMED RIZON[1], MAHMOUD MOGHAVVEMI[2,3], AND MARTYN NIGEL JAMES PALEY[4]

[1]Department of Electrical and Electronic Engineering, UCSI University, Cheras, Kuala Lumpur 56000, Malaysia
[2]Department of Electrical Engineering, University of Malaya, Kuala Lumpur 50603, Malaysia
[3]Department of Electrical Engineering, University of Science and Culture, Tehran 1461968151, Iran
[4]Department of Infection, Immunity and Cardiovascular Disease, The Medical School, The University of Sheffield, Sheffield S10 2RX, U.K.

Corresponding author: Li Sze Chow (chowls@ucsiuniversity.edu.my)

This work was supported by UCSI University under Grant REIG-FETBE-2020/013.

This work involved human subjects or animals in its research. Approval of all ethical and experimental procedures and protocols was granted by the Local Research Ethics Committee, University of Sheffield, Sheffield, U.K.

ABSTRACT This study showed an alternative and non-invasive method for measuring brainwaves using Magnetic Resonance Imaging (MRI) with a gradient echo - echo planar imaging (GE-EPI) sequence. An attempt was made to measure the axonal magnetic fields of delta and theta waves using direct detection with MRI. Time-varying brainwaves produce an axonal current which may induce a magnetic field according to the Biot-Savart law. The MR scanner can detect inhomogeneous magnetic fields caused by weak currents generated in a subject that interact with the main magnetic field, B_o, of the scanner. Fifteen healthy volunteers were scanned with closed eyes in a dark imaging room. The GE-EPI sequence was used to acquire 1500 time frame images in an axial plane on a 3.0 T Philips scanner. A Butterworth bandstop filter was applied to filter out physiological signals before the detection of brainwave signals. Fast Fourier Transform (FFT) was used to produce frequency spectra where the brainwave frequencies could be detected. Our study measured an axonal magnetic field of 1.5 ± 0.2 nT for the delta waves and 1.5 ± 0.3 nT for the theta waves. Delta waves were found in the range 1.5–4.0 Hz and theta waves in the range 4.0–6.5 Hz. The waves were found on both sides of the occipital lobe, temporal lobe, and hippocampus. We detected more theta waves (2.1% of the brain slice with 5 mm thickness) than delta waves (1.5% of the brain slice with 5 mm thickness). PLCC for the $\%|\Delta S/S_{eq}|$ between the delta and theta waves was 0.7584 at $p = 0.001$ significance level and 95% confidence level. We also applied Short Time Fourier Transform (STFT) with epoch lengths of 3.85 s, 7.7 s, and 30.8 s. But the appearance of brainwave signals was not as clear as using FFT over the entire imaging duration.

INDEX TERMS Theta wave, delta wave, brainwave, axonal magnetic field, Fourier transform.

I. INTRODUCTION

The study of neurological phenomena, specifically brainwaves is an ongoing trend in research with a lot of potential uses. Brainwaves are fluctuations of periodic activity within certain groups or populations of neurons [1]. They are related to different states of brain activity such as wakefulness or the different stages of sleep. Brainwaves can be categorized as being caused by an external stimulus, called evoked activity, or independent of eternal stimuli, called spontaneous activity. Brainwaves can be classified as background or transient [2], [3]. Background brainwaves are assumed to occur continuously during an electroencephalogram (EEG) or magnetoencephalogram (MEG) recording. They are usually found by breaking up the recorded signals into epochs of about 30 s long [4]–[6]. The transient brainwaves only

The associate editor coordinating the review of this manuscript and approving it for publication was Vishal Srivastava.

TABLE 1. Categories of brainwave and their frequency range.

Brain-wave	Frequency (Hz)		
	Jae-Hwan *et al.* [7]	Koudelková *et al.* [8]	Lim *et al.*[9]
gamma	30–50	> 30	> 30
beta	13–29.99	13–30	12–30
alpha	8–12.99	8–13	8–12
theta	4–7.99	4–8	4–8
delta	0.2–3.99	0.5–4	0.5–4

occur at specific instances and last for a short period of time. For example, mu waves and lambda waves last about 5–15 s [4], [5].

There are five conventionally recognized categories of background brainwaves according to their frequencies: alpha waves, beta waves, gamma waves, delta waves, and theta waves. There are some slight variations in the frequency range of these brainwaves according to different research groups. Table 1 shows a few examples of brainwave categories.

It is generally agreed that gamma waves are the highest frequency of brainwaves though have the least amplitude. Gamma waves were only detected recently compared to other brainwaves because they were mistaken for white noise in early experiments [8]. Beta waves are linked to higher-order thought, such as concentration and immersion [10]. Wakefulness or more specifically resting state while not concentrating on activities is commonly associated with alpha waves. Alpha waves have been characterized as a ''bridge'' between the conscious and unconscious minds that help people relax [11]. A study concluded that individuals with anxiety disorder have higher alpha waves in the frontal lobe and parietal lobe compared to healthy individuals [7]. Compared to alpha and beta waves, theta waves have a larger relative amplitude. They are synonymous with daydreaming, relaxing, or sleeping. Theta waves are often linked to having deep or raw feelings. Sleep and low brain activity (though not as low as delta waves) have both been linked to theta waves [11]. Delta waves are brainwaves that have the lowest frequency compared to other brainwaves. Delta waves are linked to deep sleep and meditation [12]. Delta waves were also discovered during low-level brain function and when performing continuous attention tasks [11]. A recent study also found the delta waves in awake individuals with a normal operating regime of neocortical circuits [12] or cognitive processing [13].

Brainwaves can be detected via several methods. The most common methods of brainwave detection are using EEG and MEG. EEG measures electrical potentials in the brain using electrodes placed on the scalp. These electrical potentials are produced by pyramidal cells, which are a type of neuron with a long dendrite arm on one side of the cell body. When a pyramidal cell is activated, it can create a net electric dipole in one direction. The combined activation of billions of other pyramidal cells on the cortex of the brain produces an electrical potential large enough to be detected by the EEG electrodes [14]. MEG records neuronal activity by using magnets to detect magnetic fields generated by neurons in the brain. The operating principle of MEG is based on Ampere's law, which states that a magnetic field is generated around a conductor carrying a current that is directly proportional to the current inside the conductor. Following Ampere's right-hand law, the magnetic field radiates outward from the conductor length. The above methods however have a few limitations. Since the signals from the scalp are distorted and the electrical potentials are very small, EEG can only detect neuronal activity generated by the outermost layer of the brain [15]. Due to the weak magnetic fields generated by neurons in subcortical regions of the brain, MEG can only detect the magnetic fields produced by neurons in the sulcal walls of the brain [15].

The background brainwaves are defined by a broadband frequency range and do not have a specific waveform shape. However, Sih *et al.* showed that they could be modelled as sinewaves [2]. The transient brainwaves were found with a specific waveform in EEG recordings. The mu waves have a ''mu'' shape; lambda waves have a sawtooth or triangular waveform [2]–[5]. Therefore, Fourier transformation into the frequency domain could identify the brainwave signals within a specific frequency band. Short Time Fourier Transform (STFT) is commonly used to investigate the presence of the brainwaves [4], [5], [16]. It uses a short epoch length for the Fourier transform to show changes of frequency components throughout the imaging or signal recording. Different epoch lengths were used in the STFT depending on the application. Sachdev *et al.* used an epoch length of 1 s to find delta wave in wakefulness [12]. Huang *et al.* used an epoch length of 30 s to detect abnormal slow wave activity in patients with mild traumatic brain injury [16]. Baker *et al.* used an epoch length of 5 minutes to study Mild Cognitive Impairment (MCI) [5]. However, the disadvantage of STFT is the frequency resolution decreases with epoch length which reduces the accuracy.

An alternative novel method of detecting brain signals is direct neuronal detection (DND) [17]. The axon of a nerve cell can be modelled as a wire, and when current flows through it, following the Biot-Savart law, a transient magnetic field will be produced around the axon. A magnetic resonance imaging (MRI) scanner produces magnetic fields which interact with protons to produce an image. The transient magnetic fields generated by the brain could also interfere with the magnetic fields produced by the MRI scanner. The resultant magnetic field could have a different magnitude and phase, depending on the location of the axon relative to the acquisition slice during imaging. Hence, the neuronal activity could cause a signal change in the MR image [18]. Using visual stimuli, DND was able to detect neuronal activity that was evoked by visual stimuli in the optic nerves, the visual cortex, and corpus callosum [18], [19]. The signal changes were found in magnitude images but not in phase signals [17].

This study aimed to measure the brainwaves using the direct detection method based on the MR signal modulation [17] caused by the axonal magnetic fields induced by the spontaneous brainwave axonal currents. The MR scanner can detect inhomogeneous magnetic fields caused by the molecules in a subject that interact with the main magnetic field, B_0, of the scanner [20]. We attempted to detect the delta and theta waves and estimate their axonal magnetic fields.

II. METHODOLOGY

A. MRI DATA

The data acquisition was performed in the Academic Unit of Radiology, University of Sheffield, UK, with ethical approval granted by the local research ethics committee. MR images were acquired using a gradient echo – echo planar imaging (GE-EPI) sequence on a 3.0 T Philips scanner. The scanning parameters were a short TR = 77 ms, TE = 30 ms, voxel size = 1.8 mm × 1.8 mm × 5 mm, matrix dimension = 128 × 128, field of view (FOV) = 230 mm, number of frames = 1500. The 1500 images were acquired on a single axial slice acquired through the eyeballs and optic nerve. A total of 15 healthy volunteers (10 females and 5 males, aged between 20 and 60) took part in the study, where the image acquisition was performed in a dark room. We ensured that the volunteers were not claustrophobic in the MRI scanner and not mentally or physically disturbed by the imaging acoustic sound. The volunteers were scanned with their eyes closed in a relaxed state in a dark imaging room. Therefore, alpha waves were expected in the relaxed state; or theta waves if the volunteers were drifting off to sleep or awake in a very deep relaxed state of mind. If the volunteer fell asleep during imaging, delta waves were expected.

B. FAST FOURIER TRANSFORM (FFT)

According to electromagnetic theory, spontaneous brainwaves in axons will produce a spontaneous magnetic field in the order of 10^{-9} T around the axons [17]. If the spontaneous magnetic field lies along the same axis with the B_0 field of the MR scanner, it will produce a minute field inhomogeneity during imaging, which will cause the signal changes that vary over the time in the similar frequency with the brainwave signals.

Matlab R2019b, MathWorks, was used for the image processing. According to Shannon's sampling theorem, the highest detectable frequency is half of the sampling frequency, which is the Nyquist frequency or folding frequency [21]. Since the GE-EPI images were acquired with TR = 77 ms, the sampling frequency, f_s, of the axial images was 13 Hz. Therefore, the Nyquist frequency was 6.5 Hz, which was also the highest detectable frequency from our datasets. Therefore, our study is only targeted to detect the delta and theta waves only.

We extracted the signal intensity of each pixel for 1500 times frames represented by a discrete signal, $x_{ij}(n)$ for $n = 1, 2, \ldots, 1500$ in the time domain, where i denotes the x-coordinate and j denotes the y-coordinate of the pixel. Then, the discrete Fourier transform coefficients for each pixel, $X_{ij}(k)$, was produced according to Eq. (1):

$$X_{ij}(k) = \sum_{n=0}^{N-1} x_{ij}(n)\, e^{-j\frac{2\pi kn}{N}} \tag{1}$$

where $N = 1500$ which is the total number of data samples, k is the discrete frequency index.

Next, the one-sided amplitude spectrum for the signal intensity for each pixel, $S_{ij}(k)$, in the frequency domain was calculated using Eq. (2):

$$S_{ij}(k) = \begin{cases} \frac{1}{N}\left|X_{ij}(0)\right|, & k = 0 \\ \frac{2}{N}\left|X_{ij}(k)\right|, & k = 1, \ldots N/2 \end{cases} \tag{2}$$

The one-sided amplitude spectrum was plotted over the frequency axis in hertz by converting the frequency index k to f (Hz) using the relation $f = kf_s/N$. Next, the one-sided amplitude spectrum as a function of frequency, $S_{ij}(f)$, was used to identify the presence of brainwaves within the expected range of frequencies. $S_{ij}(f)$ was produced using the Fast Fourier Transform (FFT) function in MATLAB.

Let S_{eq} denotes $S_{ij}(0)$ which is the DC value or equilibrium signal at 0 Hz, and ΔS denotes the changes in the spectrum due to the brainwave signal. The percentage of signal change with respect to the equilibrium signal, $\%|\Delta S/S_{eq}|$, is given by Eq. (3) in relation to the echo time, TE, and the axonal magnetic field, δB_{ax} [17]:

$$\%|\Delta S/S_{eq}| = 100\left[1 - \mathrm{e}^{-\mathrm{TE}(\gamma|\delta B_{ax}|)}\right] \tag{3}$$

where $\gamma = 42.58$ MHz/T is the gyromagnetic ratio for 1H. The $\%|\Delta S/S_{eq}|$ can be measured from the one-sided amplitude spectrum. Then, the axonal magnetic field, δB_{ax}, can be calculated using Eq. (4):

$$|\delta B_{ax}| = -ln\left[1 - \frac{\%|\Delta S/S_{eq}|}{100}\right] / (TE\gamma) \tag{4}$$

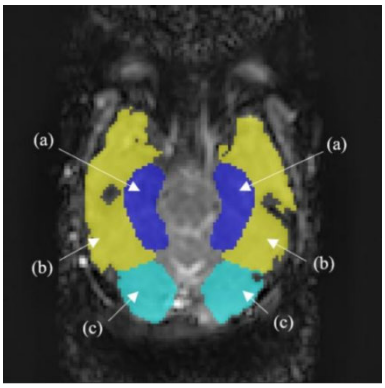

FIGURE 1. The selected ROIs for brainwave analysis include (a) hippocampus, (b) temporal lobe, and (c) occipital lobe, on both sides of the brain.

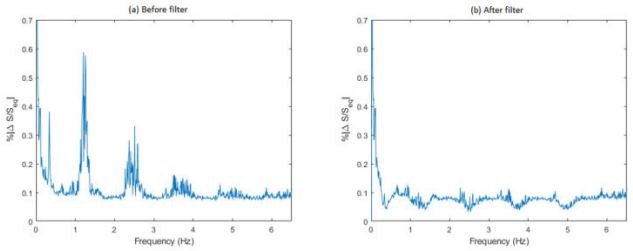

FIGURE 2. Frequency spectra from dataset 3: (a) before filtering and (b) after filtering the physiological signals.

C. REGION OF INTEREST (ROI)

The brainwave analysis was performed for the temporal lobe, occipital lobe, and hippocampus on both hemispheres, as shown in Fig. 1. The shape and location of the selected brain regions were determined by referring to a database of MR images [21]. The frontal lobe was excluded from the analysis because the GE-EPI images have poor signal intensity in this region due to ghosting and susceptibility artifacts. It was also noticed that not all regions of the brain or skull were equally visible. Therefore, these regions of low signal intensity were excluded from the analysis.

A MATLAB function was used to convert the DICOM grayscale images into a binary image, where 1 represented the pixels with acceptable MR signal intensity and 0 represented the pixels with low MR signal intensity, which were excluded from further analysis. A threshold value of 0.3 or 30% of the maximum signal intensity of the image was used to distinguish between high and low signal intensity. It was observed that those pixels with signal intensity below the threshold of 0.3 did not vary much in signal level over the time frames. The binary image was superimposed on six regions (hippocampus, temporal lobe, and occipital lobe on both hemispheres). The chosen ROIs with good MR signals are shown in Fig. 1. There are some ''holes'' in these chosen ROIs because pixels with poor MR signal intensity (binary 0) have been excluded.

D. FILTER FOR PHYSIOLOGICAL SIGNALS

Physiological signals should be removed before the detection of the brainwave signals. In the frequency spectra, the physiological signals appeared as large spikes with $\%|\Delta S/S_{eq}|$ of about 0.6%, as shown in Fig. 2 (a). The physiological signals include heartbeat and respiration signals, which are typically found at around 12–20 beats per minute (0.2–0.33 Hz) and 60–100 beats per minute (1.0–1.67 Hz) respectively [22], [23]. In this particular dataset shown in Fig. 2 (a), the respiration signal was centered at 0.3 Hz and the heartbeat signal was centered at 1.2 Hz. Besides these, their harmonics also appear in the spectra. The number of harmonics varies across different datasets, between 3 to 5 harmonics with decreasing amplitude. They obstruct the detection of the brainwave signals which are found to be in the 0.1% range. Therefore, a Butterworth bandstop filter was applied to remove all the harmonics of the physiological signals. The Butterworth filter was used because it has a very low ripple rate and the gradual drop off of the filter from the passband to the stopband matches well with the shape of the physiological signals shown in Fig. 2 (a).

The original Butterworth filter function in MATLAB produces a stopband attenuation typically between 40 to 60 dB below the passband range in the frequency spectra. The peak of the physiological signals is about 20 times (or 16 dB) higher than the mean of the other signals. Therefore, the original Butterworth filter produces an attenuation, which looks like a valley centered at the middle of the stopband range.

Therefore, the MATLAB Butterworth filter function was rescaled to adjust the stopband attenuation, A_s, to a similar amplitude level to the background noise. We applied a second order bandpass digital Butterworth filter with a transfer function given by Eq. (5):

$$H_B(z) = G\left(\frac{\sum_{i=0}^{M} b_i z^{-i}}{1 + \sum_{j=1}^{N} a_j z^{-j}} - 1\right) + 1 \tag{5}$$

where b_i and a_j are the $(M+1)$ numerator and N denominator coefficients of the filter respectively, and G is the overall gain of the filter. The coefficients b_i and a_j were calculated using the MATLAB Butterworth filter function. The gain G was calculated using Eq. (6):

$$G = \frac{A_s'}{A_s} \tag{6}$$

where A_s is the original stopband attenuation of the Butterworth filter and A_s' is the modified stopband attenuation calculated using Eq. (7):

$$A_s' = \frac{S_p}{S_{mean}} \tag{7}$$

where S_p is the physiological signal and S_{mean} is the mean signal calculated over the frequency range of 3.0 to 5.0 Hz. Both A_s' and G were calculated for each spectrum during the filtering process for each physiological signal. This process was repeated for the other prominent harmonics of the heartbeat and respiration signals. The filtered signal was then inspected. If the resulting frequency response attenuated too much or too little of the physiological signal, the value of G is further fine tuned by multiplying it with a constant between 0.5 and 1.5 until a satisfactory result was obtained. The filtering result of Fig. 2 (a) is shown in Fig. 2 (b).

E. BRAINWAVE DETECTION

After the physiological signals were filtered from the frequency spectra, the remaining signal could consist of brainwaves and background noise. Since the brainwaves can be modelled as a sine wave, triangle wave or sawtooth wave, they will appear as a ''spike'' in a high-resolution frequency spectrum. The signal-to-noise ratio (SNR) of the spike was calculated. The signal value was taken from the peak of the spike, while the noise signals were taken from the mean signals across the frequency spectra between 3.0–5.0 Hz to

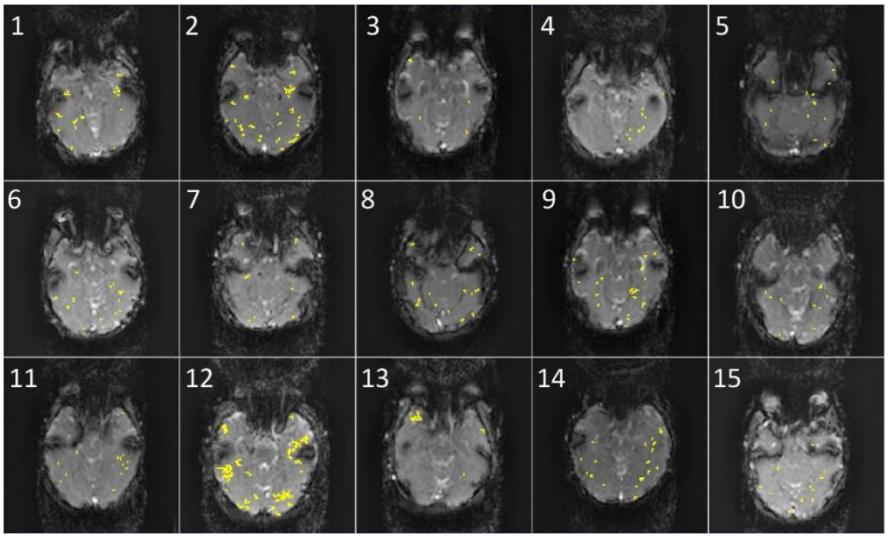

FIGURE 3. The significant pixels with delta waves for 15 datasets.

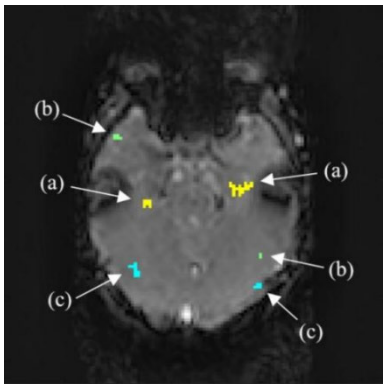

FIGURE 4. The location of six clusters with significant delta waves in both sides of the (a) hippocampus, (b) temporal lobe, and (c) occipital lobe, taken from dataset 2.

avoid any residuals from the physiological signals. It was observed that the spectra amplitude between 3.0–5.0 Hz consisted of background noise. It is more accurate to calculate a mean noise level using a broader range of frequencies instead of a specific point in the spectra. A "spike" could only be considered as a meaningful signal if it has a SNR larger than 2. However, SNR 2 could be due to any random signals. Therefore, we chose a higher SNR 3 as a minimum requirement to detect the presence of brainwave signals.

Our in-house MATLAB function was programmed to automatically search through all the voxels in the temporal lobe, occipital lobe, and hippocampus for any potential delta waves between 1.5–4.0 Hz and theta waves between 4.0–6.5 Hz. Although delta waves are between 0.5 to 4.0 Hz, our analysis excluded the range between 0.5–1.5 Hz to avoid any false "spike" from the residual physiological signals and their harmonics. The filtering process in removing the physiological signals (Fig. 2 (b)) could potentially remove any delta wave signals within the stopband of the filter. Therefore, we chose frequencies ranging between 1.5–4.0 Hz for delta wave detection.

After identifying the voxels that contained peaks with SNR ≥ 3 for the brainwave frequency ranges, those voxels that appeared adjacent to each other were considered as a significant cluster of brainwave signals. This cluster must have at least 2 voxels. The frequency spectra of all the voxels within a significant cluster were averaged to produce a cluster frequency spectrum. The rest of the random or standalone voxels were excluded.

For each of the six regions in Fig. 1, the significant cluster region with the highest percentage of signal changes, $\%|\Delta S/S_{eq}|$, and axonal magnetic field δB_{ax} was recorded. The cursor function of MATLAB was used to find the frequency, $\%|\Delta S/S_{eq}|$, and δB_{ax} of the brainwave signals. Then, the SNR of the spike of the brainwave signals was calculated. Next, the percentage of voxels that containing the brainwave signals over one brain slice was calculated. The quantitative analyses were repeated for all the datasets.

F. STATISTICAL TESTS

We performed two types of statistical tests to assess the interclass and intraclass correlation. Pearson linear correlation coefficient (PLCC) was used to evaluate the interclass correlation of $\%|\Delta S/S_{eq}|$ between the delta and theta waves. One-way Analysis of Variance (ANOVA) was used to evaluate the intraclass mean values between 15 datasets. ANOVA analysis was performed for $\%|\Delta S/S_{eq}|$ for the delta and theta waves across 15 datasets.

G. SHORT TIME FOURIER TRANSFORM (STFT)

We also performed the STFT for one dataset to compare the result with the FFT over the whole imaging duration. The FFT was performed over 1500 time frames, which is 115.5 s. We used an epoch length of 30.8 s from 400 time frames to perform STFT. Three STFT spectra and spectrograms were calculated to compare with the FFT results. We also

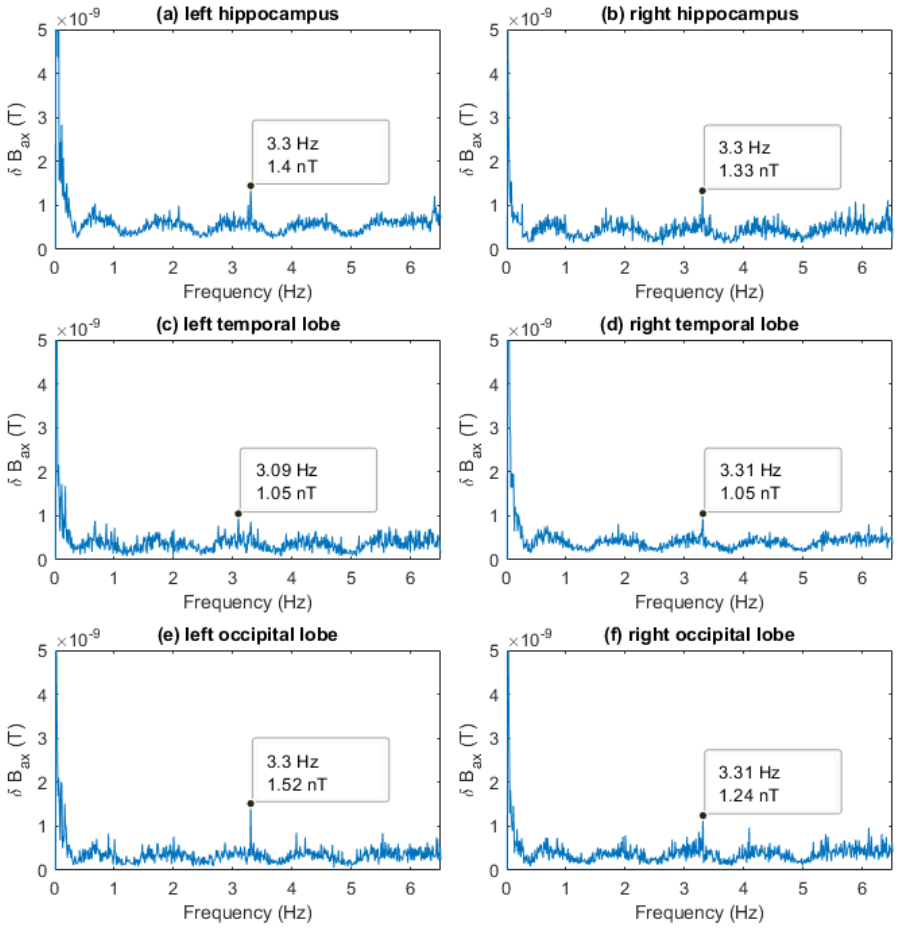

FIGURE 5. Frequency spectra of delta waves corresponding to the highlighted clusters in Fig. 4 in the regions of (a) left hippocampus, (b) right hippocampus, (c) left temporal lobe, (d) right temporal lobe, (e) left occipital lobe, and (f) right occipital lobe.

investigated a shorter epoch length of 3.85 s with 50 time frames, and 7.7 s with 100 time frames.

III. RESULTS

A. DELTA WAVES

After the physiological signals were filtered out, the significant pixels containing delta wave signals whose SNR was equal or larger than 3 are shown in Fig. 3 for all the datasets. Delta waves were found in the temporal lobe and occipital lobe. It was observed that some volunteers exhibited more delta waves than others. Dataset 2 was used to demonstrate the frequency spectra of the delta waves. Only one cluster was chosen from each of the six regions as highlighted in Fig. 4. These clusters were chosen based on the criteria of the largest cluster with the largest spike of delta wave frequency. First, the FFT was calculated for each pixel in a cluster using the time series signal intensities. Then the mean value of all the pixels' frequency spectra was calculated and shown in Fig. 5 for each of the six regions.

B. THETA WAVES

Similarly, after filtering the physiological signals, the significant pixels containing theta waves are shown in Fig. 6 for all the datasets. Theta waves were also found in the occipital lobe, temporal lobe, and hippocampus. Again, it was observed that some volunteers exhibited more theta waves than other volunteers. By comparing Fig. 3 and Fig. 6, there were more significant pixels related to theta waves than delta waves. Dataset 5 was used to demonstrate the frequency spectra of theta waves. Only one cluster was chosen from each of the six regions as highlighted in Fig. 7. These clusters were chosen based on the criteria of the largest cluster with the largest spike of theta wave frequency. The frequency spectra for each region are shown in Fig. 8, which were produced with the same method for Fig. 5.

C. QUANTITATIVE VALUES

The quantitative values of the magnetic field δB_{ax} for the delta waves and theta waves are recorded in Table 2 and Table 3 respectively. The detected brainwave frequencies with their corresponding δB_{ax} from the spectrum are recorded for each dataset in both tables. The delta waves detected in our study were between 1.5–3.6 Hz, with the δB_{ax} between 1.1–1.9 nT and, as recorded in Table 2. The theta waves were between 4.2–6.5 Hz, with the δB_{ax} between 1.1–2.1 nT,

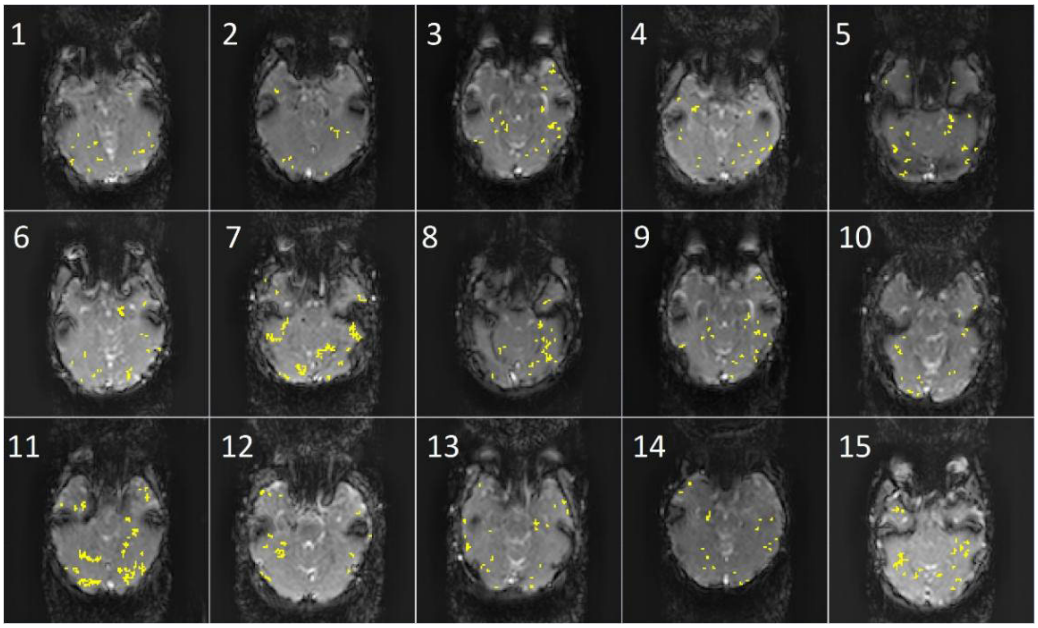

FIGURE 6. The significant pixels with theta waves for 15 datasets.

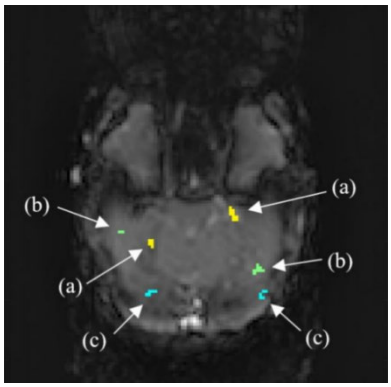

FIGURE 7. The location of six clusters with significant theta waves in both sides of the (a) hippocampus, (b) temporal lobe, and (c) occipital lobe, taken from dataset 5.

as recorded in Table 3. We also calculated the percentage of pixel clusters that contained significant brainwave signals over one brain slice, as recorded in both tables.

Table 4 records the mean $\%|\Delta S/S_{eq}|$, mean axonal magnetic field δB_{ax}, mean SNR, and percentage of brain slice for the delta waves and theta waves. The mean δB_{ax} was 1.5 ± 0.2 nT for delta waves and 1.5 ± 0.3 nT for theta waves respectively. The SNR was measured for the peak of δB_{ax} in the frequency spectra as explained earlier in the Methodology section.

D. STATISTICAL TESTS

The Pearson linear correlation coefficient (PLCC) for $\%|\Delta S/S_{eq}|$ between the delta and theta waves was 0.7584 at $p = 0.001$ significance level and 95% confidence level. It shows that $\%|\Delta S/S_{eq}|$ for delta and theta waves have a similar range of signal changes with a positive correlation. One-way

TABLE 2. Quantitative values of the delta waves (1.5–4.0 Hz) for 15 datasets.

Dataset	f (Hz)	$\%\|\Delta S/S_{eq}\|$	δB_{ax} (nT)	% of brain slice
1	1.9	0.18	1.4	1.8
2	3.3	0.17	1.3	3.9
3	3.5	0.22	1.7	0.4
4	3.3	0.23	1.8	0.6
5	1.6	0.19	1.5	0.7
6	2.1	0.14	1.1	0.9
7	2.5	0.23	1.8	0.6
8	3.6	0.18	1.4	1.2
9	3.5	0.20	1.6	1.8
10	1.9	0.22	1.7	0.5
11	2.0	0.20	1.6	0.8
12	2.5	0.15	1.2	6.3
13	1.5	0.24	1.9	0.9
14	1.6	0.18	1.4	1.6
15	1.7	0.18	1.4	0.8

ANOVA box plots of means and variances for the 15 datasets of delta and theta waves are shown in Fig. 9(a) and Fig. 9(b) respectively. The mean $\%|\Delta S/S_{eq}|$ of the delta waves were statistically significant different between the 15 datasets as determined by one-way ANOVA ($F(14,47) = 2.1054$, $p = 0.029$). The mean $\%|\Delta S/S_{eq}|$ of the theta waves were also statistically significant different between the 15 datasets as determined by one-way ANOVA ($F(14,59) = 2.6477$, $p = 0.0047$).

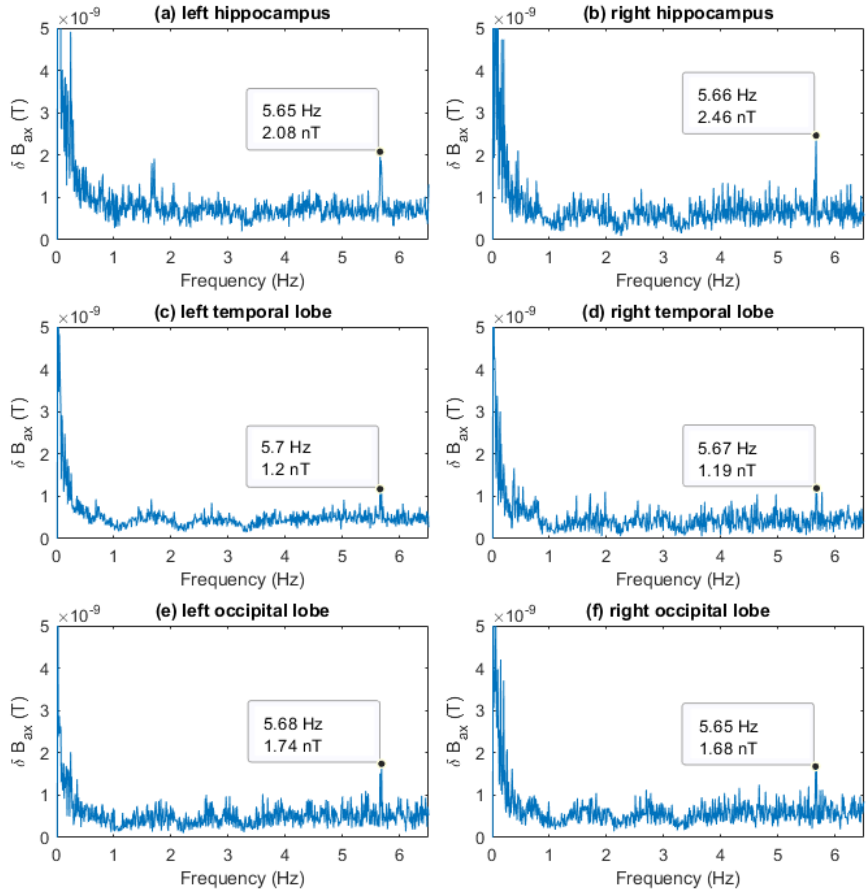

FIGURE 8. Frequency spectra of theta waves corresponding to the highlighted clusters in Fig. 7 in the regions of (a) left hippocampus, (b) right hippocampus, (c) left temporal lobe, (d) right temporal lobe, (e) left occipital lobe, and (f) right occipital lobe.

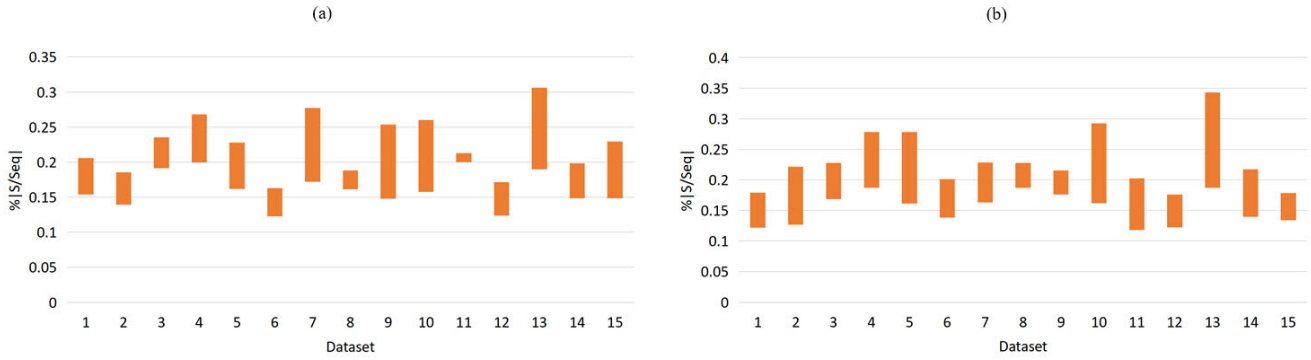

FIGURE 9. One-way ANOVA box plot of means and variances of 15 datasets for (a) delta waves and (b) theta waves.

E. SHORT TIME FOURIER TRANSFORM (STFT)

Fig. 10 shows the STFT spectrogram produced using an epoch length of 30.8 s (400 time frames) for the left and right hippocampus taken from the ROI indicated in Fig. 7 (a). From the 1500 time frames, the data were divided into three intervals of 30.8 s each. The corresponding STFT spectra for each interval are shown in Fig. 11. The 5.7 Hz signal was observed in all the intervals in the left hippocampus in both Fig. 10 (a) and Fig. 11 (a). However, it was only observed in the third interval in the right hippocampus in Fig. 10 (b) and Fig. 11 (b). We further investigated shorter epoch length of 3.85 s (50 time frames) and 7.7 s (100 time frames) as shown in Fig. 12. However, the 5.7 Hz was hardly noticeable in these spectrograms.

IV. DISCUSSION

Our detection method is based on the finding of a significant peak in the frequency spectra within the expected range of

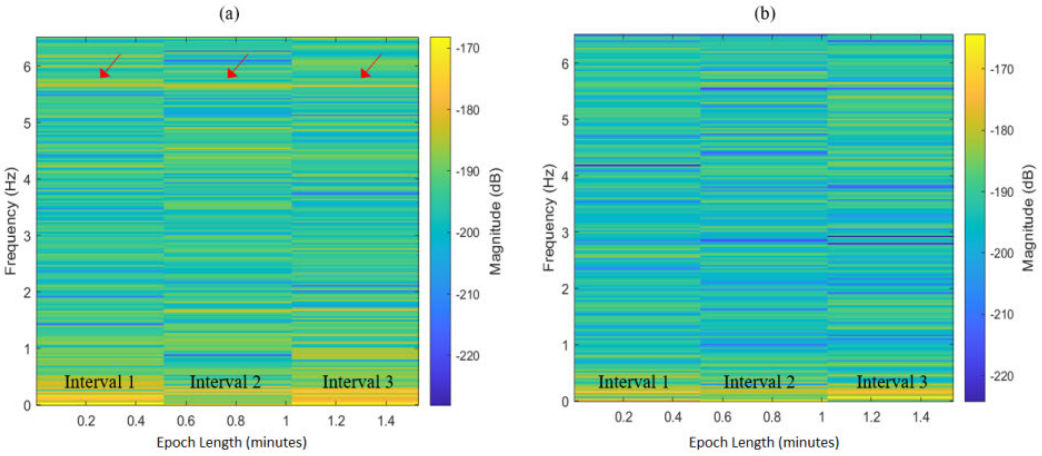

FIGURE 10. The STFT spectrogram of the (a) left hippocampus and (b) right hippocampus, taken from the ROI indicated in Fig.7 (a). The arrows in (a) indicate the appearance of 5.7 Hz across the three intervals.

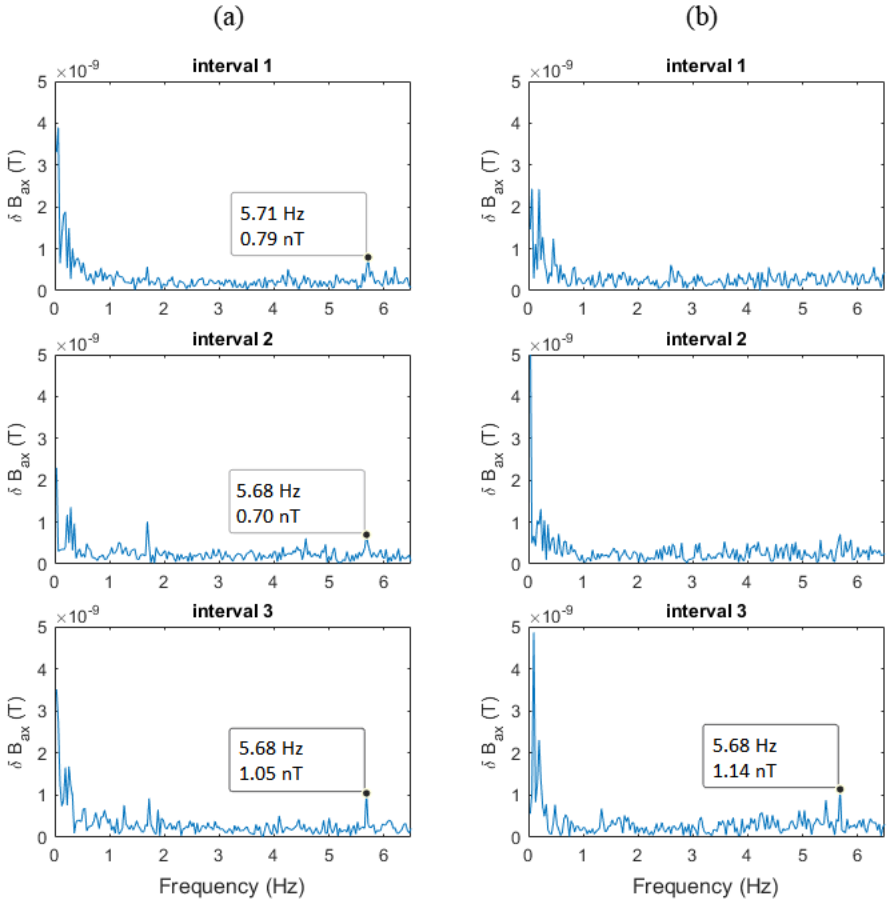

FIGURE 11. The STFT spectra corresponding to Fig. 10 for the (a) left hippocampus and (b) right hippocampus.

brainwaves frequencies. We have ensured that the brainwave signals must possess SNR equal to or larger than 3 as shown in all the frequency spectra in Fig. 5 and Fig. 8. SNR $\geq$ 3 was chosen to ensure that the spike was not due to random noise. Any random pixels with a peak were excluded. Only those pixels adjacent to each other in a cluster were considered, where the average of the frequency spectra for all adjacent pixels within the cluster was computed to produce the results shown in Fig. 5 and Fig. 8. The prominent physiological frequencies below 1.5 Hz were also excluded to avoid any false detection related to physiological signals. The appearance of a broad sinusoidal wave in the frequency spectra in Fig. 5 was due to an artifact from the Butterworth filter in the attempt to adjust the stopband

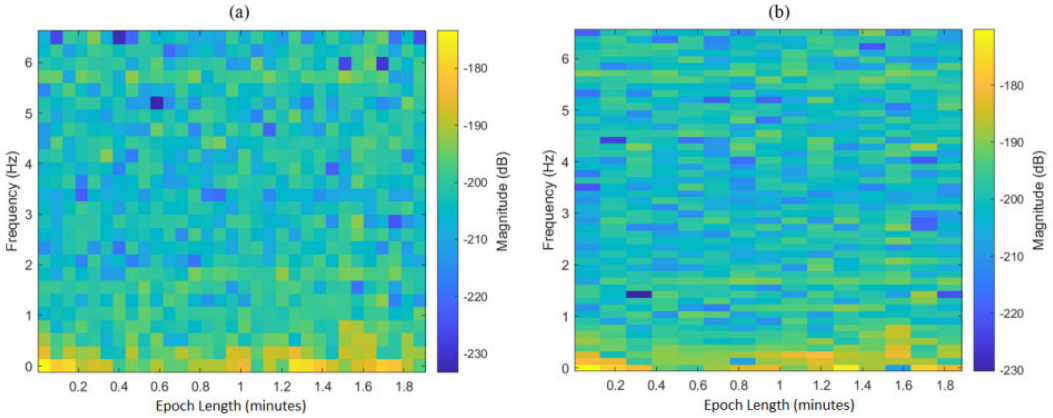

FIGURE 12. The STFT spectrogram of the left hippocampus taken from the ROI indicated in Fig. 7 (a) produced using epoch length of (a) 3.85 s (50 time frames) and (b) 7.7 s (100 time frames).

TABLE 3. Quantitative values of the theta waves (4.0–6.5 Hz) for 15 datasets.

Dataset	f (Hz)	$\%\lvert\Delta S/S_{eq}\rvert$	δB_{ax} (nT)	% of brain slice
1	4.2	0.17	1.3	1.2
2	5.4	0.17	1.3	0.9
3	5.8	0.20	1.6	2.2
4	6.0	0.23	1.8	1.5
5	5.7	0.22	1.7	1.6
6	4.6	0.17	1.3	1.3
7	5.8	0.19	1.5	4.2
8	6.5	0.20	1.6	1.8
9	5.9	0.19	1.5	1.9
10	5.6	0.23	1.8	1.1
11	6.3	0.17	1.3	6.1
12	5.0	0.14	1.1	1.7
13	6.0	0.27	2.1	1.7
14	5.3	0.17	1.3	1.4
15	5.2	0.15	1.2	2.6

TABLE 4. The mean $\%\lvert\Delta S/S_{eq}\rvert$, mean δb_{ax}, mean SNR, and percentage of the brain region for the delta waves and theta waves.

Signal type	Mean $\%\lvert\Delta S/S_{eq}\rvert$	Mean δB_{ax} (nT)	Mean SNR	% of brain slice
Delta waves (1.5–4.0 Hz)	0.2 ± 0.03	1.5 ± 0.2	3.3 ± 0.3	1.5 ± 1.5
Theta waves (4.0–6.5 Hz)	0.2 ± 0.04	1.5 ± 0.3	3.3 ± 0.4	2.1 ± 1.3

attenuation, A_s', to a similar level to the background noise. The original spectrum before the filtering process does not contain the broad sinusoidal wave. Anyway, it does not affect the detection of significant spikes from the brainwave signals. Further investigation is required to improve the Butterworth filter in a future study.

Both the delta waves and theta waves had a similar mean magnetic field of 1.5 nT, which agree with the literature values [17]. The percentage of brain regions detected with brainwave signals was quite low at only 1.5 ± 1.5 % for the delta waves and 2.1 ± 1.3 % for the theta waves. This percentage is only considered for a brain slice with 5 mm thickness. It is understood that brainwave signals vary quickly in time depending on the thought process or mental state of the volunteers during imaging. Therefore, it was not surprising that a small percentage of brain regions with significant delta waves and theta waves were found within a brain slice.

In Fig. 3 and Fig. 6, some volunteers exhibited more delta or theta waves compared to others. There are two possible reasons. First, every individual has different brain activity at any time. Even if the same volunteer repeats the imaging, it is possible to find different clusters of brainwave activation during different episodes of imaging. Second, if there was any involuntary slight movement during imaging, it may affect the continuity of brainwave fluctuation. The GE-EPI sequence is a fast-imaging sequence which required only 115.5 s (about 2 minutes) with a very short repetition time. The volunteers were advised not to move during imaging. As we managed to detect brainwave signals in all the volunteers, we believe that the volunteers did not move during the short imaging duration.

Referring to Fig. 3 and Fig. 6, both delta waves and theta waves were found in similar brain regions, mainly the temporal and occipital lobes. Earlier studies demonstrated the presence of delta waves with sleep [21], loss of consciousness [21], or disease processes [24], [25]. But a recent study showed that the delta waves in these regions were thought to correspond to normal waking brain activity and cognition tasks [12], [13]. Therefore, the ultimate trigger of delta waves is still unknown. Theta waves are thought to correspond to decreased stress when found in the occipital lobe region [6] or correspond to a background process involved in memory processing when found in the temporal lobe [26] and hippocampus [27]. Since all the volunteers

were being scanned while lying down without being given any cognitive tasks, it is logical to find more theta waves (2.1 ± 1.3%) than delta waves (1.5 ± 1.5 %) in the volunteers.

Our finding of delta waves in the temporal and occipital lobes corroborates with research findings using intracranial EEG (icEEG), a form of EEG that uses electrodes implanted within the brain to detect EEG signals [12]. Our finding of theta waves in the temporal lobe also agrees with another icEEG study, where they found that theta waves, specifically at 5 Hz, were observed prominently in the frontal and temporal lobes of the brain [26]. Besides this, in a study using a neurofeedback device to manipulate power levels of brainwaves, it was found that an increase in theta waves in the occipital lobe for patients with generalized anxiety disorder correlated with reduced symptoms of generalized anxiety disorder [6]. Our finding of theta waves in the hippocampus shows the existence of hippocampal theta oscillations which could be a result of the traveling waves that move along the hippocampus in a posterior-anterior direction [28].

The PLCC demonstrated positive correlation of signal changes, $\%|\Delta S/S_{eq}|$, between delta and theta waves. One-way ANOVA analysis demonstrated a statistically significant difference between 15 datasets for both delta and theta waves. In other words, the signal changes, $\%|\Delta S/S_{eq}|$, between 15 volunteers were significantly different, showing that individuals experienced different amplitudes of brainwave signals.

Our studies have investigated the presence of brainwaves using both FFT over the entire imaging duration and STFT over shorter epoch lengths. The STFT spectrogram demonstrated the presence of brainwaves which appear and vanish quickly. Whereas the FFT over the entire imaging duration provided an accumulated result over the imaging period. Therefore, our findings showed that FFT over the entire imaging period is more robust than STFT in detecting brainwave signals. We have evaluated the robustness of our method by applying it over 15 datasets which demonstrated consistent results as shown in Tables 2-4.

The frontal lobes were excluded in our study due to low signal intensity and ghosting artifacts found in the GE-EPI sequence. Although part of the frontal lobe called the orbital gyrus was visible in the GE-EPI images, no brainwaves signals were found in this region in our datasets. Some of the physiological signals from the circle of Willis and the subarachnoid space were superimposed onto the orbital gyrus due to a ghosting artifact. Large physiological signals were found in the corrupted region of the frontal lobe obstructing detection of possible brainwave signals which have much lower amplitude.

The study of brainwaves may provide new insights into the medical field. They can potentially be used as an alternative diagnosis or treatment assessment. For example, one study showed that Attention-deficit/hyperactivity disorder (ADHD) patients with a low alpha peak frequency (APF) in their EEG recordings were more likely to fail in responding to stimulant medication, methylphenidate (MPH) [29]. In another study, the quantity and location of slow-wave brain activity detected by MEG recordings were able to distinguish between the control group, patients with schizophrenia, and patients with affective disorders [30]. In patients with mild traumatic brain injury (mTBI), Huang *et al*. found that slow brainwave activity in the prefrontal cortex suggested personality change, difficulty focusing, and affective capacity symptoms. The detection of such brainwaves was linked to depression in patients without mTBI [16]. EEG recordings were used in another study to predict whether patients with mild cognitive impairment (MCI) will develop Alzheimer's disease [5].

Our study showed an alternative and non-invasive method for measuring brainwaves using the novelty of direct detection MRI with a GE-EPI sequence. It has an advantage over invasive methods with implanted electrodes such as icEEG. MRI can also potentially detect brainwaves across the entire brain instead of limited regions near the scalp as in the conventional MEG or EEG methods. The GE-EPI sequence uses single radio-frequency (RF) pulses in combination with readout gradient reversal [31]. Therefore, a short TR can be achieved, resulting in fast image acquisition. Fast imaging is essential in capturing the fast-varying and transient brainwaves. The sampling time for each GE-EPI image is typically the repetition time, TR. Therefore, a shorter TR will allow a wider frequency bandwidth for brainwave detection. The 77 ms TR used in this study has limited the possible detection of brainwaves to delta and theta waves only. Future studies could explore a shorter TR using parallel imaging to allow higher frequency signals to be detected. The direct detection with GE-EPI sequence also has an advantage over blood oxygenation level dependent functional MRI (BOLD fMRI) because it does not rely on the secondary response of blood oxygenation levels that occur after the evoked field. Instead, it relies on the fast-varying magnetic field changes induced by the axonal currents of spontaneous brainwaves. However, it still has the disadvantages of a GE-EPI sequence including ghosting artifacts in the frontal lobe region and low signal intensity in certain regions of the brain.

V. CONCLUSION

This study has detected delta waves and theta waves on 15 datasets of GE-EPI images from 15 volunteers using direct detection and FFT on MR images. Brainwaves were detected as significant peaks in the frequency spectra averaged from a cluster of pixels adjacent to each other in the temporal lobe, occipital lobe, and hippocampus. We measured axonal magnetic fields of about 1.5 nT for both delta waves and theta waves. We found more theta waves (2.1%) than delta waves (1.5%) from a brain slice. Rapid acquisition, wideband functional MRI can potentially provide a new method to investigate brainwaves non-invasively.

ACKNOWLEDGMENT

The authors would like to thank the Academic Unit of Radiology, The University of Sheffield, U.K., for providing the GE-EPI images for this study.

REFERENCES

[1] X. Jia and A. Kohn, "Gamma rhythms in the brain," *PLoS Biol.*, vol. 9, no. 4, Apr. 2011, Art. no. e1001045.

[2] G. C. Sih and K. K. Tang, "Sustainable reliability of brain rhythms modeled as sinusoidal waves with frequency–amplitude trade-off," *Theor. Appl. Fract. Mech.*, vol. 61, pp. 21–32, Oct. 2012.

[3] C.-S. Hung, S. Sarasso, F. Ferrarelli, B. Riedner, M. F. Ghilardi, C. Cirelli, and G. Tononi, "Local experience-dependent changes in the wake EEG after prolonged wakefulness," *Sleep*, vol. 36, no. 1, pp. 59–72, Jan. 2013.

[4] J. C. Ehlen, F. Jefferson, A. J. Brager, M. Benveniste, and K. N. Paul, "Period-amplitude analysis reveals wake-dependent changes in the electroencephalogram during sleep deprivation," *Sleep*, vol. 36, no. 11, pp. 1723–1735, Nov. 2013.

[5] M. Baker, K. Akrofi, R. Schiffer, and M. W. O. Boyle, "EEG patterns in mild cognitive impairment (MCI) patients," *Open Neuroimag. J.*, vol. 2, pp. 52–55, Aug. 2008.

[6] M. Dadashi, B. Birashk, F. Taremian, A. A. Asgarnejad, and S. Momtazi, "Effects of increase in amplitude of occipital alpha & theta brain waves on global functioning level of patients with GAD," *Basic Clin. Neurosci.*, vol. 6, no. 1, pp. 14–20, 2015.

[7] J.-H. Cho, H.-K. Lee, K.-R. Dong, H.-J. Kim, Y.-S. Kim, M.-S. Cho, and W. K. Chung, "A study of alpha brain wave characteristics from MRI scanning in patients with anxiety disorder," *J. Korean Phys. Soc.*, vol. 59, no. 4, pp. 2861–2868, Oct. 2011.

[8] Z. Koudelková, M. Strmiska, and R. Jašek, "Analysis of brain waves according to their frequency," *Int. J. Biol. Biomed. Eng.*, vol. 12, pp. 202–207, Oct. 2018.

[9] S. Lim, M. Yeo, and G. Yoon, "Comparison between concentration and immersion based on EEG analysis," *Sensors*, vol. 19, no. 7, p. 1669, 2019.

[10] P. A. Abhang, B. W. Gawali, and S. C. Mehrotra, "Technical aspects of brain rhythms and speech parameters," in *Introduction to EEG- and Speech-Based Emotion Recognition*. Amsterdam, The Netherlands: Elsevier, 2016, pp. 51–79.

[11] M. Roohi-Azizi, L. Azimi, S. Heysieattalab, and M. Aamidfar, "Changes of the brain's bioelectrical activity in cognition, consciousness, and some mental disorders," *Med. J. Islamic Republic Iran*, vol. 31, no. 1, pp. 307–312, Dec. 2017.

[12] R. N. S. Sachdev, N. Gaspard, J. L. Gerrard, L. J. Hirsch, D. D. Spencer, and H. P. Zaveri, "Delta rhythm in wakefulness: Evidence from intracranial recordings in human beings," *J. Neurophysiol.*, vol. 114, no. 2, pp. 1248–1254, Aug. 2015.

[13] T. Harmony, "The functional significance of delta oscillations in cognitive processing," *Frontiers Integrative Neurosci.*, vol. 7, p. 83, Dec. 2013.

[14] E. K. S. Louis *et al.*, *Electroencephalography (EEG): An Introductory Text and Atlas of Normal and Abnormal Findings in Adults, Children, and Infants*. Chicago, IL, USA: American Epilepsy Society, 2016.

[15] M. Proudfoot, M. W. Woolrich, A. C. Nobre, and M. R. Turner, "Magnetoencephalography," *Pract. Neurol.*, vol. 14, no. 5, pp. 336–343, 2014.

[16] M.-X. Huang, S. Nichols, D. G. Baker, A. Robb, A. Angeles, K. A. Yurgil, A. Drake, M. Levy, T. Song, R. McLay, and R. J. Theilmann, "Single-subject-based whole-brain MEG slow-wave imaging approach for detecting abnormality in patients with mild traumatic brain injury," *NeuroImage, Clin.*, vol. 5, pp. 109–119, Jan. 2014.

[17] L. S. Chow, G. G. Cook, E. Whitby, and M. N. J. Paley, "Investigating direct detection of axon firing in the adult human optic nerve using MRI," *NeuroImage*, vol. 30, no. 3, pp. 835–846, Apr. 2006.

[18] L. S. Chow, G. G. Cook, E. Whitby, and M. N. J. Paley, "Investigation of MR signal modulation due to magnetic fields from neuronal currents in the adult human optic nerve and visual cortex," *Magn. Reson. Imag.*, vol. 24, no. 6, pp. 681–691, Jul. 2006.

[19] L. S. Chow, G. G. Cook, E. Whitby, and M. N. J. Paley, "Investigation of axonal magnetic fields in the human corpus callosum using visual stimulation based on MR signal modulation," *J. Magn. Reson. Imag.*, vol. 26, no. 2, pp. 265–273, 2007.

[20] K. Möllenhoff, A.-M. Oros-Peusquens, and N. J. Shah, "Introduction to the basics of magnetic resonance imaging," in *Molecular Imaging in the Clinical Neurosciences*. Totowa, NJ, USA: Humana Press, 2012, pp. 75–98.

[21] R. Avram, G. H. Tison, and K. Aschbacher, "Real-world heart rate norms in the health eHeart study," *NPJ Digit. Med.*, vol. 2, p. 58, Jun. 2019.

[22] A. Sapra, A. Malik, and P. Bhandar. *Vital Sign Assessment*. StatPearls Publishing. Accessed: Jul. 31, 2020. [Online]. Available: https://www.ncbi.nlm.nih.gov/books/NBK553213/

[23] L. Tan and J. Jiang, *Digital Signal Processing: Fundamentals and Applications*, 3rd ed. San Diego, CA, USA: Academic, 2018.

[24] N. Gaspard, L. Manganas, N. Rampal, O. A. C. Petroff, and L. J. Hirsch, "Similarity of lateralized rhythmic delta activity to periodic lateralized epileptiform discharges in critically ill patients," *JAMA Neurol.*, vol. 70, no. 10, pp. 1288–1295, Aug. 2013.

[25] P. Gloor, G. Ball, and N. Schaul, "Brain lesions that produce delta waves in the EEG," *Neurology*, vol. 27, no. 4, pp. 326–333, 1977.

[26] D. M. Groppe, S. Bickel, C. J. Keller, S. K. Jain, S. T. Hwang, C. Harden, and A. D. Mehta, "Dominant frequencies of resting human brain activity as measured by the electrocorticogram," *NeuroImage*, vol. 79, pp. 223–233, Oct. 2013.

[27] J. E. Kragel, S. VanHaerents, J. W. Templer, S. Schuele, J. M. Rosenow, A. S. Nilakantan, and D. J. Bridge, "Hippocampal theta coordinates memory processing during visual exploration," *eLife*, vol. 9, p. e52108, Mar. 2020.

[28] H. Zhang and J. Jacobs, "Traveling theta waves in the human hippocampus," *J. Neurosci.*, vol. 35, no. 36, pp. 12477–12487, Sep. 2015.

[29] M. Arns, M. A. Vollebregt, D. Palmer, C. Spooner, E. Gordon, M. Kohn, S. Clarke, G. R. Elliott, and J. K. Buitelaar, "Electroencephalographic biomarkers as predictors of methylphenidate response in attention-deficit/hyperactivity disorder," *Eur. Neuropsychopharmacol.*, vol. 28, no. 8, pp. 881–891, Aug. 2018.

[30] B. S. Rockstroh, C. Wienbruch, W. J. Ray, and T. Elbert, "Abnormal oscillatory brain dynamics in schizophrenia: A sign of deviant communication in neural network?" *BMC Psychiatry*, vol. 7, no. 1, p. 44, Dec. 2007.

[31] M. Markl and J. Leupold, "Gradient echo imaging," *J. Magn. Reson. Imag.*, vol. 35, no. 6, pp. 1274–1289, 2012.

LI SZE CHOW received the B.Eng. degree in telecommunication from the University of Malaya, Malaysia, in 2001, and the M.Sc. degree in data communication and the Ph.D. degree in electrical and electronic engineering from The University of Sheffield, U.K., in 2003 and 2006, respectively.

From 2006 to 2010, she was a Research Associate with the Academic Unit of Radiology, The Medical School, The University of Sheffield. She worked as a Senior Lecturer with SEGI University, from 2012 to 2014, then at the University of Malaya, from 2014 to 2017. She is currently an Assistant Professor with UCSI University, Kuala Lumpur, Malaysia. Her research interests include medical image processing with the magnetic resonance (MR) images for the optic nerve and brainwave studies. She also works on the chest X-ray images (CXR) for the classification of pneumonia using convolutional neural network (CNN). She received her Chartered Engineer (CEng) status from the Institution of Engineering and Technology (IET), U.K., in 2016.

REUBEN GEORGE received the B.Eng. degree in electrical and electronics engineering from UCSI University, Kuala Lumpur, Malaysia, in August 2021, where he is currently pursuing the Ph.D. degree in engineering.

In 2018, he took an internship as a Radio Frequency Engineer at UCE Sdn. Bhd., for four months. Then in 2019, he got a placement as an IoT Intern at Atilze Digital Sdn. Bhd., for four months. He also worked as a Research Assistant at the UCSI University for four months, in 2020, and another four months, in 2021, during the semester break. His research interests include electronic engineering, brain imaging, and digital signal processing.

Mr. George is a Graduate Engineer with the Board of Engineers Malaysia.

MOHAMED RIZON received the B.Eng. and M.Eng. degrees in electrical and electronics engineering from the University of Tokushima, Japan, in 1993 and 1995, respectively, and the Ph.D. degree from the Department of Computer Science and Intelligent System, Oita University, Japan, in 2002. From 1995 to 1997, he was a Software Engineer with the System LSI Laboratory, Mitsubishi Electric Corporation, Itami, Japan. In 1997, he moved to the University of Malaya, Malaysia. He was the Head of the Biomedical Engineering Department, University of Malaya. He was a Professor of biomedical technology with King Saud University, Saudi Arabia, in 2010. He has served for MIEC, Fuzhou University, China, in 2019. He is currently a Professor with the Department of Electrical and Electronics, UCSI University, Malaysia.

MAHMOUD MOGHAVVEMI received the B.Sc. degree in electronics from the State University of New York at Buffalo, Buffalo, NY, USA, the M.Sc. degree in electrical engineering from the University of Bridgeport, Bridgeport, CT, USA, and the Ph.D. degree in electrical engineering from the University of Malaya, Kuala Lumpur, Malaysia.

He was a Test and Design Engineer with CTI Electronics Corporation, Fairfield, CT, USA, and the Director of the Informatics School of Engineering, Kuala Lumpur. He joined the Department of Electrical Engineering, University of Malaya, where he is currently serving as a Full Professor. He is a reviewer for several distinguished journals in his field of expertise. He is also the Founder and the Director of the Center for Research in Applied Electronics, University of Malaya. His contributions to the scientific community are evident by more than 30 patents and more than 250 refereed journals articles and conference papers.

MARTYN NIGEL JAMES PALEY received the B.Sc. degree in physics and the Ph.D. degree from Nottingham University, U.K., in 1976 and 1981, respectively, and the M.Ed. degree from The University of Sheffield, U.K., in 2003.

He has been employed as a Combustion Engineer with Rolls-Royce Aero-Engines, Derby, U.K., from 1976 to 1978; a Senior Physicist with Kodak Research Laboratories, Harrow, U.K., from 1981 to 1983; the MRI Techniques Section Leader with Picker International Ltd., Wembley, U.K., from 1983 to 1989; the MR Sequence Development Manager with Picker International Inc., Cleveland, OH, USA, from 1989 to 1991; a Senior Lecturer with the University College London, U.K., from 1991 to 1997; and the Professor of MR Physics with The University of Sheffield, U.K., from 1997 to 2017. He is currently the Emeritus Professor of biomedical imaging with The University of Sheffield. He has been involved in the research of nuclear magnetic resonance (NMR) and magnetic resonance imaging and spectroscopy (MRI/S) since 1973. He has published over 200 articles, book chapters, and nine patents.